IEEE Access
Multidisciplinary | Rapid Review | Open Access Journal

Received January 7, 2020, accepted February 10, 2020, date of publication February 21, 2020, date of current version March 3, 2020.

Digital Object Identifier 10.1109/ACCESS.2020.2975621

A Layered Subtree Scheme for Multicast Communications in Large-Scale Elastic Translucent Optical Networks

MEHDI TARHANI, (Member, IEEE), MORAD KHOSRAVI EGHBAL, AND MEHDI SHADARAM
Department of Electrical and Computer Engineering, The University of Texas at San Antonio, San Antonio, TX 78249, USA

Corresponding author: Mehdi Tarhani (mehdi.tarhani@utsa.edu)

This work was supported in part by Janey and Dolf Briscoe Endowment at the University of Texas at San Antonio.

ABSTRACT To exploit the capacity introduced by elastic optical networks, efficient algorithms must be developed. Efficient modulation techniques have limited reach, so for distant destination nodes, the regeneration of a signal at a few intermediary nodes along the lightpath can effectively reduce the spectrum utilization and offset the extra cost, in terms of overall transceiver use, introduced by enabling the regeneration. In the context of multicast provisioning, although regeneration can be complex, it, in turn, due to its flexibility, further emphasizes the advantage of tree based routing over serving individual destinations. In this paper, we investigate the problem of routing, modulation level, spectrum allocation, and regenerator placement (RMSA-RP) for multicast provisioning, which, to the best of our knowledge, has not been previously addressed in the literature. Accordingly, we present a networking model through comprehensive integer linear programming, jointly enabling a routing method based on a subtree scheme as well as assigning a few nodes as regenerators of the signal. By means of an algorithm, we also propose a scalable framework to address RMSA-RP when the network is in operation. This algorithm implements a dynamic and automatic geographic partitioning of the destination nodes and then forms the corresponding subtree structures. Constraints taken into account include wavelength contiguity, wavelength continuity, and light splitting that affects the reach of the modulation techniques. Extensive simulation results show that the model can effectively support a greater number of demands without increasing transceiver use.

INDEX TERMS Elastic optical networks, modulation, multicast, regeneration placement, routing, spectrum allocation, subtree.

I. INTRODUCTION

In recent years, many emerging applications, such as advanced weather forecasting, self-driven cars, industrial automation, online social media, and video streaming, have been facilitated using technologies such as Internet of Things and artificial intelligence. High line rates and low latency are among the base requirements of these applications. For the wireless segment, fifth generation (5G) mobile communication was started recently, and for fiber-based transmission systems, these requirements have provoked extensive research to realize cost-effective networks with higher capacity [1], [28]. Elastic optical networks (EONs) have been proposed in recent years to support higher transmission bit rates and disparate bandwidth needs by using the optical spectrum more efficiently and flexibly than its counterpart, wavelength division multiplexing (WDM) [2], [3]. The key elements characterizing EONs include adaptive transmission, a flexible grid, and intelligent client nodes [4], which allow a trade-off between reach and spectral efficiency as well as dynamic networking and superchannel base transmissions [5].

While EONs introduce new flexibilities, they also pose new restrictions on networking, which altogether necessitate a reinvestigation of all previously developed WDM-based networking patterns [4]. Two fundamental restrictions include the so-called wavelength contiguity and wavelength continuity: the former dictates that all frequency slices employed for a given lightpath be adjacent within each link, and the latter prohibits wavelength conversion along the signal path until it reaches its destination [3].

Routing, modulation level, and spectrum allocation, (RMSA), is the principal problem faced when determining the best lightpath between any source-destination pair requested by incoming demands to the network in such a way

The associate editor coordinating the review of this manuscript and approving it for publication was Farhana Jabeen Jabeen.

as to accommodate the maximum number of demands within the lifetime of the network [6]. To achieve this end, an algorithm must manage resource utilization and its distribution. More specifically, an EON allows a dynamic selection of modulation techniques based on signal quality requirements while more spectrally efficient techniques such as 16QAM have shorter reaches (i.e., the distance that the signal can travel without serious physical impairment). Furthermore, a shorter distance in terms of the number of hops between the transmitter and receiver implies fewer links and hence requires fewer resources. At the same time, to establish a lightpath, an algorithm should consider uniform resource utilization as a secondary policy to avoid creating bottlenecks in the network, in which case it creates costly transmissions for upcoming connection requests [7], [8].

An important class of applications requires transferring the same data from one source to more than one destination, a topology known as multicast networking as opposed to one-to-one or unicast transmission. Multiple studies [9]–[12] have shown that serving such requests jointly through a tree-based topology, in which the source is the root and the destinations are the leaves, potentially saves more resources than serving the destinations separately and independently. This follows from the fact that generally a signal travelling toward a destination can be split to feed another close destination, thereby eliminating the need for establishing a separate connection [7]. Although effective, the full tree structure may not be the ultimate solution. A tree with a large number of destination nodes usually implies a high number of connected links, and this translates into lower possibility of finding a spectrum that is available throughout the tree (wavelength continuity) to serve the demand. The second inefficiency manifests itself when a close destination to the source has to adopt the same spectrally inefficient modulation technique that is necessary for a farther destination. Additionally, since splitting the light in a tree further limits the reach of the modulation techniques, inefficient modulation techniques are the only choice for the joint provision of multiple destinations [13]–[16]. A newly suggested alternative, a subtree scheme, alleviates these drawbacks of a full tree-based structure.

Compared to all-optical EONs, translucent EONs can provide flexibility: they permit regeneration of the transient signal at a few intermediary nodes along its path, which may or may not be capable of modulation conversion depending on the technology that is adopted [1]. If regeneration includes modulation conversion, it is more likely to employ spectrally efficient transmissions, resulting in less resource utilization. In terms of the transmission cost, less spectrum requirements lead to lower number of required transceivers at the source and destinations, which may compensate for the extra transceivers dedicated to the regeneration of the signal. Although this regeneration can complicate the RMSA problem, incorporating this flexibility in multicast provisioning may be advantageous and, to the best of our knowledge, has not been addressed in the literature.

In this paper, we formulate an integer linear programming problem to model a new subtree-based transmission structure that supports multicast networking. We assume that modulation conversion is possible at dynamically selected nodes. Due to the highly complex nature of ILP and to meet the stringent time requirements of solving the RMSA problem when the network is in operation, we further propose a fast and efficient heuristic algorithm. As the second contribution of this paper, we examine the effect of regeneration conversion on the provisioning capacity and transmission cost of the network. To do so, under the same configuration, we disable regeneration and then compare the results in terms of blocking probability and transceiver use to reveal the possible benefits of each paradigm under different traffic loads and diverse network scales.

The rest of this paper is organized as follows: section II reviews the latest research in this area. Section III presents the ILP formulation and the heuristic algorithm. A numerical evaluation is summarized in section IV, and section V concludes this paper.

II. RELATED WORK

Tree-based RMSA has been studied at length [9]–[13]. In [9], an ILP formulation and a heuristic algorithm were proposed for both static and dynamic scenarios. The model in this study takes into consideration the limitation on the maximum light splitting degree (MSD) of the nodes. Ruiz and Valesco in [10] compared tree-based transmission with the independent provisioning of destinations for multicast networking and showed that the former can result in more resource savings. The research group in [11] formulated an all-optical multicasting RMSA and provided a genetic heuristic algorithm (GA) that outperforms the solutions achieved by employing the shortest path tree (SPT) algorithm. Walkowiack *et al.* proposed new ILP models and heuristics that incorporate distance adaptive transmission (DAT) and were shown to be more effective and applicable when compared with previous works, [12].

Subtree multicasting has been studied in [13]–[16]. In [13], using an ILP formulation, three basic schemes were modeled for point-to-multipoint (P2MP) transmissions: single path, tree based, and subtree-based topologies. These models treat only the routing and spectrum allocation. The results showed that the subtree scheme outperforms the other two schemes in terms of network capacity. The work [14] shows the same advantage while proposing both ILP and heuristics. These models solved the RMSA problem. The ILP model in the paper was based on precalculated paths between node pairs, which may not necessarily result in an optimal solution. In [15], it was assumed that data in each demand are accessible in more than one node in the data center network, and based on this assumption, a subtree-based solution to serve all destination nodes was provided. An ILP was employed in a static scenario and a heuristic was employed in a dynamic scenario. In [16], a light forest based on rateless network coding was employed to create set-cover trees. Both ILP and

heuristic algorithms were proposed and effective all-optical multicasting was obtained.

A number of studies have addressed both RMSA and regeneration placement (RP) [17]–[22]. It should be noted that all of these studies have addressed unicast transmission. [17] proposed a model in which RMSA-RP is resolved through solving two sub-problems: RMSA and RP. Additionally, to improve the scalability issue of the mixed integer linear programming (MILP), they implemented a recursive MILP and showed that the results are close to ideal non-recursive models. For translucent EONs, [18] provided joint RMSA-RP formulation but did not provide a heuristic algorithm for use when the network is operating. In addition, transceiver usage was not studied. In [19], RMSA-RP was solved jointly without providing any solution for large-scale networks with a high number of demands, where a fast algorithm is required. The effect of considering regeneration for unicast transmission was studied in [20]. Through ILP formulations, three network scenarios were modeled. The first scenario considered all-optical networking that does not allow regeneration of the signal at any node (i.e., all-optical bypasses). In the second scenario, regeneration of the signal was allowed and conducted in locations selected by the model based on need. The signal, however, had to maintain the same modulation level from the source to the destination. The third scenario removed this limitation by enabling optional modulation conversion at selected regenerating nodes. For each scenario, a multiobjective ILP was provided to address both the blocking probability and the transceiver use. The results showed that the third scenario was more successful in terms of both criteria in large-scale networks. [22] proposed a heuristic algorithm for treating RMSA and RP in point-to-point EONs. The issue addressed was the energy efficiency of the network: the capacity was not the main focus. The authors in [29] addressed the manycast transmission routing and spectrum allocation. However, they did not study regeneration in their work. In their routing models, they employed fiber nonlinearity models instead of experimental results to approximate the signal-to-noise ratio.

III. TRANSLUCENT MULTICASTING

A. NETWORK MODEL

In this paper, we assume a network where the nodes are connected by bidirectional fiber cables; all fiber cables are identical, and the full range of available optical spectrum in each fiber is composed of 40 contiguous frequency slices with a central wavelength spacing of 12.5 GHz. We also assume a maximum of one frequency slice per transceiver, and to transmit a signal that requires more than one frequency slice, OFDM-based superchannels are allowed. A demand for data transmission can arrive at the network at any time. A demand is denoted by $q(src, D, b)$, where src represents the source node, D represents the set of destination nodes, and b denotes the required data rate to serve the demand. The sources and destinations are distributed uniformly across the network. A request is either served or fully rejected. The requested data rate for each demand ranges from 1 to 50Gb/s. The modulation levels considered in this paper are $m(\in M) = 1, 2, 3, 4$ to signify binary phase shift keying (BPSK), quadrature phase shift keying (QPSK), 8-quadrature amplitude modulation 8QAM, and 16QAM, respectively, which can support data rates b_m up to 12.5, 25, 37.5 and 50 Gb/s per frequency slice, respectively. By default, a node employs all-optical bypass for any transient signal. However, to serve a given demand, we have the choice of assigning one or more nodes as regenerator nodes. The regeneration is assumed to be carried out through two sets of back-to-back transceivers as in [17], [20], and [22], and thus we assume we have the choice of selecting a different modulation technique than the one that is used originally at the source.

The reach of a modulation technique i.e., the maximum distance that the signal can travel without serious physical impairment, is shorter for the techniques that are more spectrally efficient. Various studies have examined this effect. In this paper, we use the values obtained in [23]. The relation that takes into account the effect of splitting the light at nodes on the reach of a modulation technique [24], [25], [16] is:

$$R(m, n) = \frac{R^m}{\log(n) + 1} \tag{1}$$

where R^m is the reach of the modulation technique m for a one-to-one transmission, $R(m, n)$ is the reach of each branch in a tree/subtree and n is the splitting order (i.e., the number of branches in the tree/subtree.); $R(m, n)$ defines the maximum length from the source to any destination node in the tree/subtree. Table 1 summarizes the resulting values for different modulation levels.

TABLE 1. Reach (in km) by the number of branches in a tree.

	$n = 1$ (one to one)	$n = 2$	$n = 3$	$n = 4$
BPSK	5000	3842	3385	3120
QPSK	2500	1920	1692	1560
8QAM	1250	960	846	775
16QAM	625	480	432	387

The number of frequency slices required for a demand with data bit rate b is the least integer equal to or greater than $(b/b_m) + 1$, where b_m is the maximum bit rate supported by the modulation technique m and one extra slice is assigned as a guard band. For instance, a demand with a required bit rate of $b = 30$Gb/s occupies 3 slices if QPSK is used for modulation: $(3 \geq (30/25) + 1)$.

B. ILP-BASED RESOURCE ALLOCATION

The ILP formulation presented in this section partitions the destinations into smaller subsets and forms a subtree to serve each subset. No two subtrees share spectrum in any link. Each node is fed through only one subtree in case the demand is served. The case where all destinations are served through one tree and the case where there is one separate path formed

to serve each destination are two special forms of a subtree. The source of the data is only one node for each demand. Depending on the geographical positions of the nodes and the distances between the source and the destinations, it may also place an intermediary node to play the role of regenerator of the signal. For simplicity in this study, we assume that regeneration at no more than one node is allowed on any subtree. To solve the RMSA-RP problem, it is possible to rely on precalculated values for some assignment decisions and then design ILP to complete the solution. This approach drastically reduces the size of the ILP. Its outcome, however, is not necessarily the optimal solution. Thus, in our model, no intervention is made, and all assignments are decided by ILP. In the context of RMSA, an ILP can be exploited in two ways. The first way is when it solves the problem for all demands in the network jointly, which requires the knowledge of all demands in advance of running. This so-called joint ILP is used for network planning. The other version, separate ILP is used for dynamic scenarios; it accepts one demand at a time and aims at RMSA with minimized resource utilization for any input demand when the previous demands have already been determined. Separate ILP is produced by a simple modification of joint ILP.

In the following, for better organization, the constants and variables of ILP are first introduced, and the equations are then arranged in sets to distinguish their functionalities.

Constants:

V : Set of the nodes in the network.
L : Set of fiber links.
Dis : Set of physical lengths of the links in L
K : Set of demands.
S : Set of frequency slices in each fiber link.
O_i : Set of outward links of node i in L.
I_i : Set of inward links of node i in L.

Variables:

${}^{d}h_j^k$: Equals 1 if link j is used for serving destination d in demand k, otherwise equals 0.

${}^{d}reg_i^k$: Equals 1 if node i is a regenerator for the signal serving destination d in demand k, otherwise 0.

${}^{d}r_j^k$: Equals 1 if link j is used for serving destination d in demand k after regeneration (if any) of the signal, otherwise equals 0.

${}^{m}_{n}\lambda_d^{k,b}$: Equals 1if modulation format m is used, in demand k, for serving destinations on a subtree with n branches which includes destination d and its root is source node, when $b = 0$, or a regenerator node, when $b = 1$. Without a regenerator, the two values will be equal.

${}^{d}_{s}z_j^k$: Equals 1 if frequency slice s in the link j is used for serving destination d in demand k, otherwise equals 0.

${}^{s}Y_j^k$: Equals 1 if slice s in link j is used in demand k, otherwise 0.

${}^{d}_{s}\Phi_b^k$: Equals 1 if slice s has been and $s-1$ has not been used to serve destination d in demand k in at least one of the links connected to the source (when $b = src$), or connected to the destination (when $b = d$), otherwise equals 0.

${}^{d_x}_{d_y}\Psi_b^k$: Equals 1 if destinations d_x and d_y are in the same subtree in demand k and the subtree root is source node, (when $b = 0$), or is a regenerator node, (when $b = 1$), otherwise equals 0.

${}^{d_x}_{d_y}c^k$: Equals 1 if lightpaths to destinations d_x and d_y in demand k share at least one link after regenerating (if any), of the signals, otherwise 0 or 1.

${}^{d_x}_{d_y}Cr^k$: Equals 1 if both destinations d_x and d_y are in the same subtree that its root is source node and the signal serving d_y has regeneration, otherwise 0.

${}^{d_x}_{d_y}\alpha^k$: Equals 1 if the signal that is received at destination d_x uses frequency slices with equal or higher indices than those for destination d_y, otherwise 0.

$$\text{Objective function: Minimize } \Big(\sum_{k\in K}\sum_{j\in L}\sum_{s\in S}{}^{s}Y_j^k\Big) \tag{2}$$

The summation in (2) considers the set of frequency slots in all of the links. ILP aims at minimizing the total amount of spectrum usage. The demand serving is subject to the following constraints:

$$\sum_{j\in O_i}{}^{d}h_j^k \le 1, \quad i \in V \tag{3}$$

$$\sum_{j\in I_i}{}^{d}h_j^k \le 1, \quad i \in V \tag{4}$$

$$\sum_{j\in O_i}{}^{d}h_j^k - \sum_{j\in I_i}{}^{d}h_j^k = \begin{cases} 0, & otherwise \\ 1, & i = src \\ -1, & i = d, \end{cases} \tag{5}$$

$${}^{d_y}_{d_x}\Psi_b^k - {}^{d_x}_{d_y}\Psi_b^k = 0, \quad d_x, d_y \in D, b \in \{0,1\} \tag{6}$$

$${}^{d}_{d}\Psi_b^k = 1 \quad b \in \{0,1\} \tag{7}$$

It should be noted that dots denote multiplication and all equations in this section are for $k \in K$ and $d \in D$ (unless stated otherwise), which are not explicitly included to save space. For each demand, (3)–(7) collectively form the subtrees to connect the source to the destinations. Equations (3) and (4) ensure that no more than one path is selected between a source and any destination. Equation (5) guarantees the existence and the connectivity of a path for each destination: if a signal comes into a node, one must go out. Equation (6) dictates that if destination d_x is in the same subtree as destination d_y, d_y is also in the same subtree as d_x.

$${}^{d_x}reg_{i_1}^k + {}^{d_y}reg_{i_2}^k + {}^{d_x}_{d_y}\Psi_0^k \le 2, \quad d_x, d_y \in D,\ i_1 \ne i_2 \in V \tag{8}$$

$$\sum_{j\in I_d} {}^{d}r_j^k - \sum_{i\in V} {}^{d}reg_i^k = 0, \tag{9}$$

$$\sum_{j\in O_d} {}^{d}r_j^k - \sum_{j\in I_d} {}^{d}r_j^k = \sum_{i\in V} reg_i^k \tag{10}$$

$${}^{d}r_j^k - {}^{d}h_j^k \le 0, \quad j \in L \tag{11}$$

$${}^{d_x}r_j^k + {}^{d_y}r_j^k \le 2 + {}^{d_x}_{d_y}c^k - {}^{d_x}_{d_y}\Psi_0^k, \quad j\in L, d_x, d_y \in D \tag{12}$$

$$2{}^{d_x}_{d_y}\Psi_1^k \le {}^{d_x}_{d_y}\Psi_0^k + {}^{d_x}_{d_y}c^k, \quad d_x, d_y \in D \tag{13}$$

Equations (8)–(13) apply the limitations on the placement of the regenerator node in each subtree. In case there is a regeneration for the signal serving d, (9)–(11) collectively label any link that is located after the regeneration by making the variable r equal to 1. Equation (12) ensures that if the variable *come* is zero for two destinations on a subtree, according to its definition, their paths after modulations do not have an overlap.

$${}^{m}_{n}\lambda_d^{k,b} R(m,n) \ge \begin{cases} \sum_{j\in L} Dis_j.({}^{d}h_j^k - {}^{d}r_j^k), & b = 0 \\ \sum_{j\in L} Dis_j.{}^{d}r_j^k, & b = 1, \end{cases} \quad m \in M \tag{14}$$

$$({}^{m}_{n}\lambda_d^{k,b} - 1)\Delta \le \begin{cases} n - \sum_{d_y\in D} ({}^{d}_{d_y}\Psi_0^k - {}^{d}_{d_y}cr^k(1-1/\Delta)), & b = 0 \\ n - \sum_{d_y\in D} {}^{d}_{d_y}\Psi_1^k, & b = 1 \end{cases} \quad m \in M, \tag{15}$$

$$2{}^{d_x}_{d_y}Cr^k \le {}^{d_x}_{d_y}\Psi_0^k + \sum_{i\in N} {}^{d_y}reg_i^k, \quad d_x, d_y \in D \tag{16}$$

$$\sum_{n\le 5}\sum_{m\in M} {}^{m}_{n}\lambda_d^{k,b} = 1, \quad b \in \{0,1\} \tag{17}$$

$${}^{m}_{n}\lambda_{d_x}^{k,b} - {}^{m}_{n}\lambda_{d_y}^{k,b} \ge {}^{d_x}_{d_y}\Psi_b^k - 1 d_x, d_y \in D, \quad b \in \{0,1\} m \in M \tag{18}$$

$${}^{b}f_d^k \ge (\lceil b/b_m \rceil + 1){}^{m}_{n}\lambda_d^{k,b}, \quad b \in \{0,1\}, m \in M \tag{19}$$

Equations (14)–(19) determine the appropriate modulation format and the required number of frequency slots for each subtree. Equations (14) and (15) filter out the modulation formats that cannot be used at a source, $b = 0$, or at a regenerator node, $b = 1$, for transmitting the signal. These two equations are linear equivalents of (1). The right side of (14) considers the length of the path in each section, and that of (15) considers the number of branches in each subtree. Equation (17) states that for each signal, only one modulation format should be selected. Equation (18) states that for all destinations in the same subtree, the same modulation format must be applied. At this point, Equation (19) is capable of calculating the number of required frequency slices on each assigned link before the regeneration, $\sum_{s\in S}\sum_{j\in O_{src}} {}^{d}_{s}z_j^k$, and after the regeneration, $\sum_{s\in S}\sum_{j\in I_d} {}^{d}_{s}z_j^k$ (which are shown by ${}^{0}f_d^k$ and ${}^{1}f_d^k$ respectively).

$${}^{d}_{s}z_j^k - {}^{d}h_j^k \le 0, \quad j \in L, \ s \in S \tag{20}$$

$$-{}^{d}reg_i^k \le \sum_{j\in O_i} {}^{d}_{s}z_j^k - \sum_{j\in I_i} {}^{d}_{s}z_j^k \le {}^{d}reg_i^k, \quad i \in V - \{src\} - \{d\}, \quad s \in S \tag{21}$$

$$(-1/2) \le 2.{}^{d}_{s}\Phi_b^k - \sum_{j\in I_b\cup O_b} {}^{d}_{s}z_j^k + \sum_{j\in I_b\cup O_b} {}^{d}_{s-1}z_j^k \le 1,$$

$${}^{d}_{0}z_j^k = 0, b \in \{src, d\}, s \in S, \tag{22}$$

$$\sum_{s\in S} {}^{d}_{s}\Phi_b^k \le 1, \quad b \in \{src, d\} \tag{23}$$

Equations (20)–(23) apply the main limitations on the assignment of frequency slots for individual subtrees. We need to ensure, by (20), that all required frequency slices will be within the transmission links that have already been assigned by (3)–(5). In particular, for a destination d, if a link j has not been selected (i.e., ${}^{d}h_j^k = 0$), then ${}^{d}_{s}z_j^k = 0$, which means that no slots on the link are assigned. In (21), each summation, with a maximum value of one, indicates whether the slot s has been selected in one of the two links on the subtree connected by node i (right summation for input links to i, and the other is for output links). In this equation, if node i is not a regenerator for the destination d (i.e., ${}^{d}reg_i^k = 0$), then for (21) to hold, the two summations must be equal, and this happens only and only if slot s has been selected in both the links or it has been selected in neither. In other words, Equation (21) states that, unless when passing through a regeneration node, the spectrum for any signal has to be the same over the entire path from the source to any destination. This is the same rule as wavelength continuity. Equations (22) and (23) force the other constraint, wavelength contiguity: In (22), summations, with the maximum value of one each, show whether, to serve d, slots s and $s-1$ have been selected in a link coming out of the source; these two summations obviously make ${}^{d}_{s}\Phi_b^k$ equal to one only and only if the left summation is one (i.e., slot s has been selected) and the other summation is zero (i.e., slot $s-1$ has not been selected). In other words, (22) checks if slice s has been used to serve destination d provided that its previous slice s–1 has not. Thus, if the number of checked slices in each link is limited to one, by (23), the only possible arrangement of employed slices within the spectrum is for them to be adjacent.

$${}^{d_x}_{s}z_j^k + {}^{d_y}_{s}z_j^k \le 1 + {}^{d_x}_{d_y}\Psi_0^k, \quad j\in L, \ s\in S, \ d_x, d_y \in D \tag{24}$$

$$\sum_{s\in S} s({}^{d_x}_{s}\Phi_{src}^k - {}^{d_y}_{s}\Phi_{src}^k) \le (1 - {}^{d_x}_{d_y}\Psi_0^k).\Delta, \quad d_x, d_y \in D \tag{25}$$

$$H_{d_y}^{d_x} \le (2 - {}^{d_x}_{d_y}\Psi_1^k - {}^{d_x}_{d_y}c^k).\Delta, d_x, d_y \in D \tag{26}$$

$$0 \le {}^{d_x}_{d_y}\alpha^k\Delta - H_{d_y}^{d_x} - \frac{1}{2} \le \Delta, \quad d_x, d_y \in D \tag{27}$$

$$H_{d_x}^{d_y} + {}^{d_y}fr^k \le (2 + {}^{d_x}_{d_y}\Psi_1^k - {}^{d_x}_{d_y}c^k - {}^{d_x}_{d_y}\alpha^k).\Delta, d_x, d_y \in D \tag{28}$$

$$0 \le {}^{s}Y_j^k\Delta - \sum_{d\in D} {}^{d}_{s}z_j^k, \quad j \in L \tag{29}$$

$${}^{s}Y_j^{k'} + {}^{s}Y_j^k \le 1, \quad j \in L \ s \in S, k', k \in K, k \ne k' \tag{30}$$

where $H_b^a = \sum_{s\in S} s({}^{a}_{s}\Phi_a^k - {}^{b}_{s}\Phi_b^k)$.

There are still some restrictions to be applied for the validity of the spectrum assignment in our scheme where both subtrees and regenerations are allowed. Equations (24)–(30) intend to avoid conflict on the allocation of frequency slots for subtrees in the same or different demands. In particular, if ${}^{d_x}_{d_y}\Psi_0^k = 0$, then for any slot s in link j, both ${}^{d_x}_{s}z_j^k$ and ${}^{d_y}_{s}z_j^k$ cannot be equal to one in (24). In other words, if two destinations are not in the same subtree, they cannot share spectrum in any link in their paths. For two destinations belonging to the same subtree, they should use exactly the same spectrum: according to (25), if ${}^{d_x}_{d_y}\Psi_0^k = 1$, then the left side of the equation must be zero, and this happens only if ${}^{d_x}_{s}\Phi_{src}^k = {}^{d_y}_{s}\Phi_{src}^k$, which means that the first slot in the frequency bands for both the destinations is the same, and as they have already been given the same number of frequency slots, they will have exactly the same frequency band. Additionally, in case the signals for either or both destinations have undergone regeneration, there are two scenarios after regeneration: if the signals are still in the same subtree, i.e., ${}^{d_x}_{d_y}\Psi_1^k = {}^{d_x}_{d_y}c^k = 1$, then these make the right side of (26) equal to zero, and again similar to (25), the left side assigns a shared spectrum for both the destinations. If they use the same link only, that is, ${}^{d_x}_{d_y}\Psi_0^1 = 0$ and ${}^{d_x}_{d_y}c^k = 1$, not a single slice can be shared: if destination d_x is using slots with higher indices than those of d_x, in which case ${}^{d_x}_{d_y}\alpha^k$ is set to one by (27), the summation in (28), which is the difference between the indices of the first slots for destinations d_x and d_y must be larger than the entire frequency band ${}^{d_y}fr^k$ for destination d_y, which in turn means that the assigned bands for destinations d_x and d_x will not have an overlap. A frequency slot in a fiber link is marked as *in use* by (29) if it has been used (or if it has been considered as a guard band for a signal). Finally, (30) guarantees that no spectrum in any specific link is used by more than one demand.

For simplicity of evaluation, we assume that no more than one regeneration is allowed per subtree. To allow more than one regeneration, some equations must be modified while the other formulas remain the same. However, these changes make the ILP more complicated. The reader should also note that since the multicast structure in this scheme is subtree and that destinations in a subtree, as opposed to in a full tree, are fewer in number and locally closer, there is a higher chance that one well-positioned regenerator node can serve all the destinations and provide resource savings.

This ILP is modified to produce a separate ILP for the dynamic scenario, which minimizes resource utilization in each demand. More specifically, all k subscriptions are removed, and (30) is replaced by $({}^{s}Y_j + {}^{s}F_j \leq 1)$, where binary variable ${}^{s}F_j$ is 1 if the frequency slot s in link j is already in use by previous demands. Also for any demand, if the separate ILP model is infeasible, then there is no possible way to assign a path to each destination from the source and thus the request is rejected.

In terms of complexity, solving the RMSA problem has been shown to be *NP* complete. Among the variables, z creates the highest number of variables ($|K|.|D|.|L|.|S|$). This is followed by h with $2.|K|.|D|.|L|$ and Φ with $2.|K|.|D|.|S|$ variables. The complexity of constraints lies in (24) with $2.|K|.|D|^2.|L|.|S|$ constraints. We should remember that we put the ILP in charge of all decisions. Furthermore, the ILP determines the need and (if any) the locations of the regenerators.

C. PROPOSED HEURISTIC ALGORITHM

When the network is in operation there is a stringent performance requirement for solving the RMSA–RP problem. To serve the maximum number of demands, the algorithm should utilize resources efficiently, which translates to using fewer links and less spectrum per link. In the EON framework, both latter conditions are satisfied by choosing paths that are short in terms of the number of links constituting the path as well as the physical length of the path. The latter arises from the fact that, in short distances, highly spectrally efficient modulation techniques can be used. Over long distances, regenerating the signal maintains the option of choosing efficient modulation techniques. However, minimizing resource utilization does not guarantee overall efficiency. In fact, the algorithm should use resources evenly across the network to avoid creating bottlenecks that might make an area either inaccessible to the rest of the network or make RMSA very costly for a portion of source–destination pairs. Lastly, when the network is under a heavy load, it is crucial for the algorithm to remain flexible and agile to find and assign resources efficiently. In this section, we design an algorithm to implement a subtree-based scheme, capable of regeneration for multicast provisioning.

To begin, we define cost C of a transmission on each link by (similar to that in [9]):

$$C = \beta d + (1 - \beta).normalized(\sum_{s \in S} z_s/|S|) \qquad (31)$$

where d represents the normalized physical length of the link, β is a tuning coefficient, S is the set of frequency slots in the link, and z_s is a binary variable that shows whether a frequency slot $s \in S$ is in use by an active demand, $z_s = 1$, or is available to use, $z_s = 0$. In other words, the summation calculates the fraction of the total frequency slots in the link that are already in use by previous demands that are still active. This equation incorporates two factors, length and availability of the link, to determine the cost: a higher link length reduces the possibility of employing an efficient modulation format, and using links that are already in heavy use by previous demands can create bottlenecks. Hence, this definition emphasizes the efficiency of the transmissions and the uniform distribution of resource utilization.

The proposed algorithm applies a subtree-based layered enhanced mechanism (SLEM) to break the problem into smaller parts: for each demand, it sorts destinations into closer and further destinations (two layers). As stated earlier, in this paper, at most one regeneration is allowed for each path.

The decision on whether regeneration may be required between each pair of the nodes in the network (e.g., the scenario where one node is the source and the other is the destination) is made once before the network operation. required. The measure is the length of the direct path between the pair, as determined by the shortest path algorithm, SPA. We assign a cutoff distance *regdis* to make this decision. Additionally, for each pair, if regeneration is required, B intermediary nodes, referred to as $RGS\,(src, d)$, are selected as the best candidates to carry out such regeneration. The selection of these candidates is solely based on resource requirements: a node i compared to node j is a better candidate for a pair *src* and d if using this node as the signal regenerator results in less link-slice consumption over the path connecting *src* to d. In other words, for each node i, the SPA is executed twice, once from the source *src* to this node i and once from this node to the destination d and then for each part, the requirements are calculated and added to find the total requirements of using node i as the regenerator. After it assigns a resource requirement to each node, it sorts the nodes based on the associated resource requirements, and m nodes with the least resource requirements will be selected as *RGS (src, d)*. These data are stored and later used in each demand to sort the destinations.

After receiving a demand in the operation phase, the algorithm generally considers destinations one at a time for the sake of resource allocation. For each destination, a path, modulation level and spectrum are assigned. The last two, however, are subject to change until all the destinations have been taken into consideration.

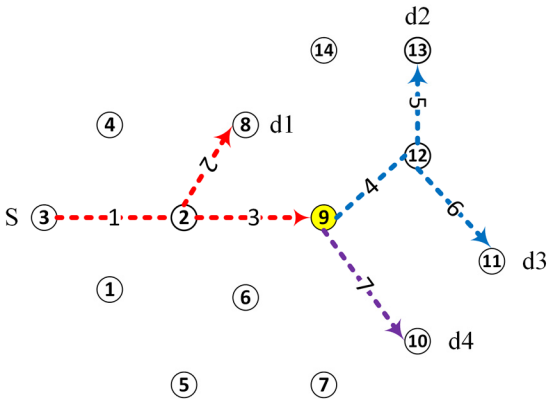

FIGURE 1. ***pst*** **and** ***sst*** **formation in SLEM.**

Resource assignment begins with routing. For each destination, SLEM finds a pool of routes, and after checking their availability, assigns the one with the least resource utilization. To search for a route, it executes SPA based on (31), and the route is returned provided that sufficient spectrum is available over the corresponding links. We define a prime subtree (*pst*) as a branch that is fed directly from the source and a secondary subtree (*sst*) as a branch that is served indirectly. For instance, in Fig. 1, there are two *sst*s and one *pst*: the red branch serves a regenerator (node number 9) and destination *d1*. One of the *ssts* (color blue) serves the destinations *d2* and *d3,* and the other (color purple) serves the node *d4*, both served by the regenerator node number 9. Additionally, in our algorithm, there are three ways to search for a path between a source and a destination, all are based on the SPA. Type *A*: the SPA is executed and then the algorithm checks to see if there is enough spectrum available (i.e., not in use by previous demands that are still active) over the path to serve *d.* Type *B*: the SPA is executed twice: once from *src* to a regenerator node and once from this node to destination *d,* and then for each segment, spectrum availability is checked. Type C involves finding a route by joining a subtree (*sst*/*pst*): to do so, the weights of all links over the subtree are initially set to zero, and then the SPA is executed to find a path. In this type, since the found path combined with the subtree form a new expanded subtree, there are more links in the new subtree, so the applicable modulation level might also be different. Therefore, the availability of the spectrum over the new subtree is examined.

To connect a source to any destination, the SLEM searches and considers a pool of paths, and after checking their availabilities, it chooses the one with the least resource requirement. In our view, this approach provides several advantages. First, under light to medium loads, all of the searched paths are available and thus the algorithm supports efficient transmission. Under heavy loads, it prioritizes serving the demand. Second, given that the paths are dynamically selected (not precalculated paths), this approach also helps to form efficient subtrees in any scenarios in terms of distribution of source and destinations in the network.

Algorithm 1 shows how the SLEM processes the RMSA-RP after receiving each demand. The input of the algorithm is a demand, and the output will be sets of *pst*s and *sst*s denoted by *PST* and *SST*, respectively. In line 1, the destinations are sorted into two sets based on the precalculated pair distances in the initial phase. We refer to the first set as the regeneration required destinations *(RRD)* and for symmetry, *NRRD* denotes the other group. At first, the *SST* and the *PST* are empty (lines 2 and 3). Line 4 makes certain that the routing will be done for any destination belonging to *RRD*. Lines 6–8 execute routing type *B* on all of the regenerator candidates belonging to *RGS (src, d)*. Lines 9–12 execute routing types *C* and *A*. If *SST* is still empty, this step is skipped. If the algorithm has found any valid path(s), the link-slice costs for the found paths are calculated, in line 16, and the one with minimum requirements is chosen as the final lightpath for the destination d. It should be noted that if this path has joined a subtree (as a result of routing type *C*), the cost not only includes the slices of the added links but also the increase in the required slices over the entire subtree due to a possible change of modulation level. In line 17, the sets *SST* and *PST* are updated: if the path was found by a type *B* routing (line 7), then one new *sst* and one new *pst* are added to their corresponding sets; if it was a type *C*, then one *sst* is replaced and no new *pst* is created. In the case of a type *A* routing, a new *sst* is added. Line 18 removes the destination *d*

Algorithm 1 Resource Allocation by SLEM

Input: demand q(s, D, b)
Output: *PSTs* and *SSTs*
1: Distribute D into *RRD* and *NRRD*;
2: Set $SST = \varnothing$;
3: *Set* $PST = \varnothing$;
4: **While** $|RRD| \neq 0$ **do:**
5: Consider a random member $d \in RRD$;
6: **for** *any member* $rgs \in RGS(s, d)$ **do:**
7: *Choiceset* ← Find a path from s to d through *rgs*;
8: **end**
9: **for** *any member* $sst \in SST$ **do:**
10: *Choiceset* ← Search for a lightpath from the root of *sst* to d by joining it;
11: *Choiceset* ← Search for a lightpath from the root of *sst* to d independently;
12: **end**
13: **if** $|choiceset| = 0$ **then:**
14: Reject the demand;
15: **end**
16: Select in *choiceset* the path with minimum cost;
17: Update *SST* and *PST*;
18: $RRD = RRD–d$;
19: Set $Choiceset = \varnothing$;
20: **End**
21: **While** $|NRRD| \neq 0$ **do:**
22: Consider a random member $d \in NRRD$;
23: **for** *any member* $sst \in SST$ **do:**
24: *Choiceset* ← Search for a lightpath from the root of *sst* to d by joining it;
25: *Choiceset* ← Search for a lightpath from the root of *sst* to d independently;
26: **end**
27: **for** *any member* $pst \in PST$ **do:**
28: *Choiceset* ← Search for a lightpath from the root of *pst* to d by joining it;
29: *Choiceset* ← Search for a lightpath from the root of *pst* to d independently;
30: **end**
31: **if** $|Choiceset| = 0$ **then:**
32: Reject the demand;
33: **end**
34: Select in *choiceset* the path with the minimum cost;
35: Update *SST* and *PST*;
36: $NRRD = NRRD - d$;
37: Set $Choiceset = \varnothing$;
38: **End**
Return;

from *RRD*. Lines 21–28 execute a similar procedure for the other group (or closer layer), i.e., those that are closer to the destination (*NRRD*).Obviously, this group enjoys more routing options because *SST* and *PST* have more members created in the previous steps for *RRD*. The algorithm treats the destinations as two different layers. The reason that routing in SLEM is first executed for the furthest layer is because, in our view, the locations of more distant destinations are the key to determining what subtrees are required. Furthermore, this approach provides more ways of connecting the source to the closer destinations, which results in a more efficient and automatic formation of subtrees for two reasons: a path from a source to a destination may eliminate the need to choose a second path from the source for another destination, and a node acting as a regenerator for a destination can act as a source for another destination in the same demand.

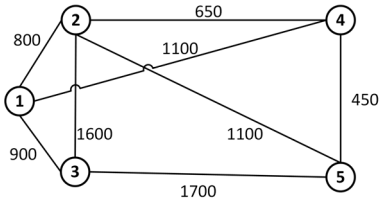

FIGURE 2. A small 5-node 8-link exemplary network.

The proposed SLEM algorithm can be extended to allow more than one regeneration per subtree. To do so, first, more than two layers are created; in the initial phase, the long paths are divided by a number greater than two. Second, in algorithm 1, routing is again executed first for the destinations in the farthest layer (from the source) and then, one at a time, for closer layers.

The time complexity for lines 1-3 is $O(|D|)$, where $|D|$ is the number of destinations per demand and the worst case complexity of lines 4-20 and 21-38 each is $|D|^2 \times N^2 \times |S|$, in which N is the number of nodes in the network and $|S|$ is the number of frequency slots per link. Therefore, the total time complexity of the algorithm is $O(|D|^2 \times N^2 \times |S|)$.

IV. PERFORMANCE EVALUATION

A. ILP-BASED EVALUATION

In this section, we first evaluate the performance of the separate ILP model presented in this paper. In this first case, the model is tested to give the blocked demands, and resource utilization per 10000 demands. The distribution and duration of the demands follows a Poisson distribution with fixed $\lambda = 10$ and an exponential distribution with $\mu = 100$, respectively.

We set the number of frequency slices at 6 per link to decrease the running time. The destinations are two nodes per demand, and selection of the source and destination nodes is random. We derive the results for the US backbone network shown in Fig. 3.

To implement the formulations, Gurobi [26] on Python is used on a computer with three cores, a 2.2 GHz speed, and 6 GB RAM.

To observe the capacity for improvement rendered by the proposed method, we also carried out the same examination

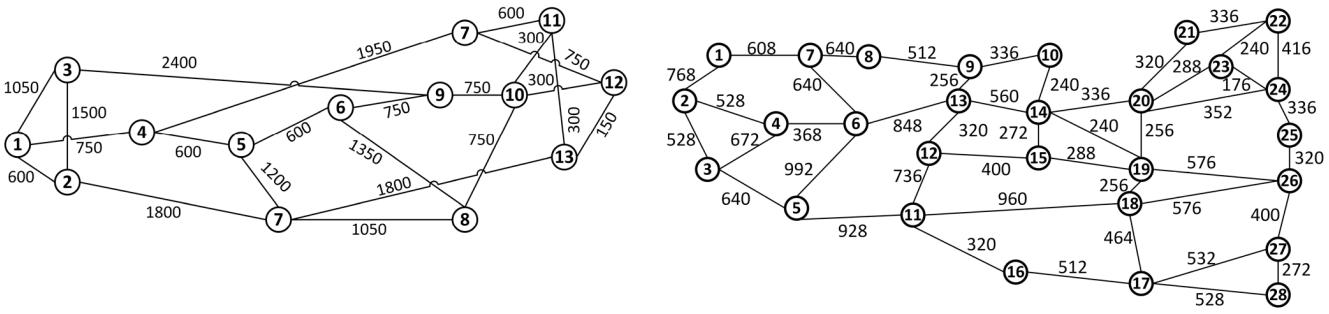

FIGURE 3. Network Topologies: (a) NSFNet network; (b) US Backbone network.

TABLE 2. Blocking probability and resource utilization.

	T	S	RS
Frequency slot usage	24.1	22.4	17.15
Blocking probability	38%	34%	12.2%
Transceiver usage	7.9	7.93	8.3

TABLE 3. Resource utilization.

	T	S	RS
Frequency slot usage	87.3	84.4	63.6
Transceiver usage	31.5	32.4	33.2

for a scenario where all the destinations are served by one tree structure as well as a scenario where the destinations are served by forming a subtree as proposed in this paper, while in both scenarios, we remove regeneration placement from the model (i.e., all-optical mode). The first scenario, which we refer to as T, can be archived simply by setting the right sides of (6) and (8) to 1. Likewise, the second scenario, which we refer to as S, is achieved by setting the right side of (8) to 1.

Table 2 shows the results. The proposed method (denoted by RS) decreases the spectrum usage by 28.8% and it increases the transceiver usage by 5 % compared to full tree scenario. It means that a large portion of the extra number of transceivers that are used for the signals regenereation are compensated for by the savings in the transceiver usage realized by employing a higher modulation format as a result of shorter transmitting distances. The blocking probability is also decreased by 25.8%. The proposed subtree scheme without regeneration, S, also has its own merits compared to the tree scenario. It decreases the blocking probability and spectrum usage by 4% and 7% respectively while the usage of the transceivers is almost the same.

For the static scenario, the ILP is loaded with a set of 4 demands in which the source and destination nodes are random. Table 3 shows the averages of the resource utilizations over 100 experiments. The results are comparable to those that were obtained for the separate ILP: the proposed model reduces bandwidth usage by 28% and 25% compared to the tree model and subtree model, respectively. Therefore, allowing a regeneration of the signal along the path by the proposed model, although complicating the resource allocation, can offer substantial savings in terms of resource usage.

B. ALGORITHM EVALUATION

In this section, we evaluate the performance of the proposed algorithm, SLEM, and its regeneration-disabled version, SLEM-RD. The criteria are the number of demands that they can serve and average transceivers used per served demand.

To make the comparison, we also measure these factors for a recent multicast algorithm, proposed in [9], named Mixed CMRSA/DMRSA (referred to as C/DMRSA for brevity). We carry out this comparison under various loads, different numbers of destinations and different network scales. In particular, we consider three network topologies: the US Backbone in Fig. 3(b), the NSFNet in Fig. 3(a), and the small network in Fig. 2. We assume 40 frequency slices per link. The distribution (arriving time) of the demands follows a Poisson distribution with fixed $\lambda = 10$ and the duration of the demands follows an exponential distribution with variable μ to represent different traffic loads. The results shown in this section are derived through simulation. We use MATLAB platform for this purpose. For any specific configuration that includes changes in the number of destination nodes or in the type of network, we run the simulation three times with 6000 demands each time and then average the outputs to ensure the accuracy of the provided results.

We first tune *regdis*, the main parameter in the SLEM. Figs. 4 and 5 show the effects of this parameter on the performance of the algorithm. This examination is conducted on the US Backbone. The destinations are five nodes per demand. It is worth noting that a very large *regdis* value, approximately 4000 km or more in this network, indicates that the SLEM selects no regeneration for any source-destination pair, is equivalent to the SLEM-RD algorithm.

One observation in Fig. 4 is that the algorithm can deliver its least blocking probability at a *regdis* of approximately 2200 km. This indicates that using regenerators can result in lower blocking probability, a conclusion that was expected. In terms of transceiver use, Fig. 5 shows a slight gradual decline while *regdis* is increasing. In comparing SLEM (*regdis* equal to 2200 km) and SLEM-RD (operating with

TABLE 4. Elapsed time (seconds) to execute different algorithms.

# of dest.		US Backbone SLEM	US Backbone SLEM-RD	US Backbone C/DMRSA	NSFNet SLEM	NSFNet SLEM-RD	NSFNet C/DMRSA	The Small 5-node Network SLEM	The Small 5-node Network SLEM-RD	The Small 5-node Network C/DMRSA
2	Ave.	0.0284	0.0194	0.0171	0.0275	0.019	0.0167	0.0206	0.0182	0.0144
	Var.	0.0001	0.000023	0.000006	0.00013	0.00002	0.0000067	0.00003	0.0000193	< e-08
5	Ave.	0.0678	0.0388	0.0285	0.0622	0.0608	0.0283	-	-	-
	Var.	0.002	0.00041	0.0000251	0.014	0.0003839	0.0000007	-	-	-

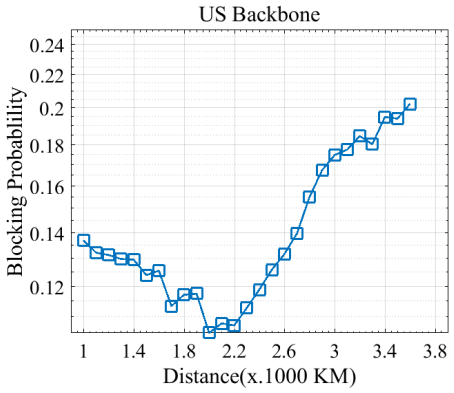

FIGURE 4. Effect of *regdis* on blocking probability.

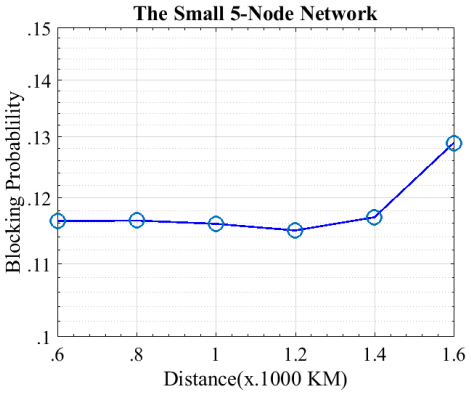

FIGURE 6. Effect of *regdis* on blocking probability.

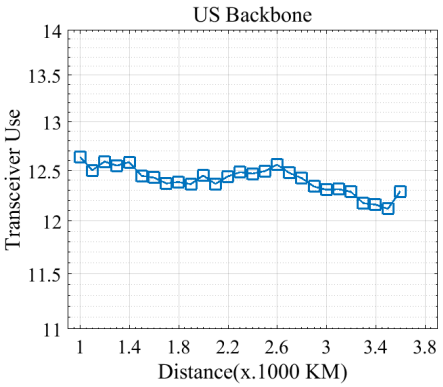

FIGURE 5. Effect of *regdis* on transceiver use.

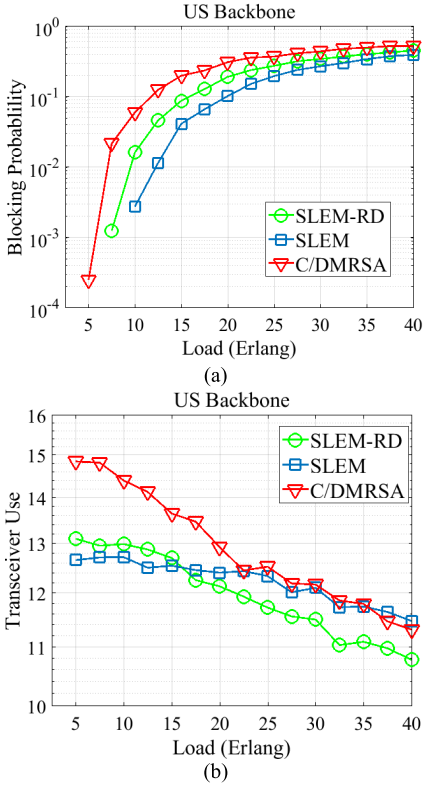

FIGURE 7. Performance comparison under various loads (5 destination nodes per demand).

regdis equal to 3600 km), there is slightly less transceiver use in the SLEM- RD, which is a consequence of its higher blocking probability. In fact, as *regdis* increases, the algorithm tends to reject more demands requiring large trees, and, thus transceiver use per served demand drops. Generally, these two graphs demonstrate that SLEM can achieve a lower blocking probability without increasing transceiver use. Fig. 6 shows the results of the same experiments for the small five-node network.

In Fig. 7 and Figs. 8(a) and 8(b), we plot the results for the US Backbone and NSFNet networks. In these simulations, we set the number of destination nodes at five. In Figs. 8(c), 8(d), 8(e), and 8(f), the algorithms serve only two destinations, to represent a small number of destinations in the US Backbone and the small 5-node network, respectively. For any algorithm, in each of these figures (7 and 8), if the load is less than a certain amount, the algorithm can serve all demands applied to the network. On the other hand, under heavy loads, all algorithms similarly reject the majority

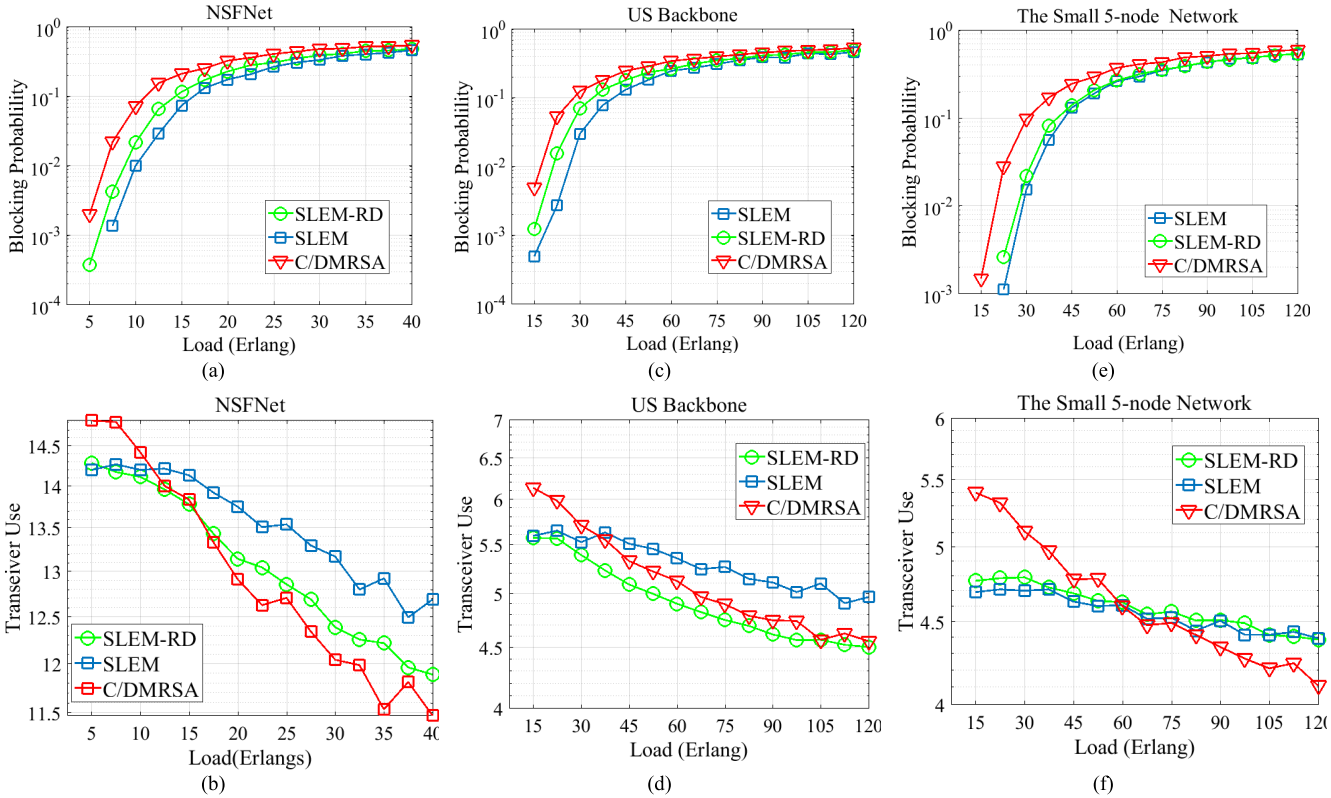

FIGURE 8. Blocking probability and transceiver use for NSFNet (a) and (b), US Backbone(c) and (d), and the small 5-node network (e) and (f), with 5, 2 and 2 destination nodes per demand respectively.

of the demands. Another observation is that, at any operational point, the SLEM outperforms the SLEM-RD, and both of these algorithms outperform C/DMRSA. For small loads, where an algorithm can manage to serve all demands, the transceiver use is less for the SLEM. For all of the algorithms, transceiver use declines when increasing the load. This is essentially because, under higher loads, the algorithms are forced to reject a portion of demands that are normally expected to be those requiring higher resources, due to either their higher requested bit rate or higher source–destination distance (physical length or number of links). Either way, this explains why the transceiver use per served demand declines faster (for C/DMRSA) where blocking probability rises in Figs. 7 and 8.

As expected, there is marked improvement achieved by the SLEM for larger networks and with higher numbers of destination nodes. In particular, Fig. 7(a) illustrates a drop of up to 10% in blocking probability, which at this operational point is equivalent to increasing the capacity of the network (the loads that can receive the same blocking probability) by up to 50%, with a negligible increase in transceiver use, as observed in Fig. 7(b). The increment in capacity is less in other cases, especially in the smaller networks.

We also examine the running time of the algorithms, as presented in Table 4. In each scenario, the C/DMRSA is faster than the SLEM and the SLEM-RD, and the SLEM has the longest execution time. All three algorithms consider each destination one at a time for the sake of resource allocation. The process is thus intrinsically serial and cannot be shortened. The difference in their running times is attributable to the C/DMRSA requiring one execution of the SPA, per destination, whereas this number is potentially higher for the SLEM/-RD. It should be noted, however, that the execution of different SPAs for the same destination in the SLEM or the SLEM-RD are independent of each other and thus are fully parallelizable. In other words, whereas parallelization cannot be applied to the C/DMRSA, it can be used in the SLEM and the SLEM-RD to reduce the execution times closer to the values for the C/DMRSA.

V. CONCLUSION

In this paper, we develope a model to solve the problem of routing, modulation level and spectrum allocation as well as regeneration placement for multicast provisioning by implementing a subtree scheme. The results of model simulations show that the model, in a dynamic scenario, can add up to 50% to the capacity of network to accommodate more demands without compromising the cost of transmission in terms of transceiver usage.

REFERENCES

[1] J. M. Simmons, *Optical Network Design and Planning*, 2nd ed. New York, NY, USA: Springer, 2014.

[2] W. Shieh, X. Yi, and Y. Tang, "Transmission experiment of multi-gigabit coherent optical OFDM systems over 1000 km SSMF fibre," *Electron. Lett.*, vol. 43, no. 3, p. 183, Feb. 2007.

[3] M. Jinno, H. Takara, B. Kozicki, Y. Tsukishima, Y. Sone, and S. Matsuoka, "Spectrum-efficient and scalable elastic optical path network: Architecture, benefits, and enabling technologies," *IEEE Commun. Mag.*, vol. 47, no. 11, pp. 66–73, Nov. 2009.
[4] O. Gerstel, M. Jinno, A. Lord, and S. J. Yoo, "Elastic optical networking: A new dawn for the optical layer?" *IEEE Commun. Mag.*, vol. 50, no. 2, pp. s12–s20, Feb. 2012.
[5] J. Armstrong, "OFDM for optical communications," *J. Lightw. Technol.*, vol. 27, no. 3, pp. 189–204, Feb. 1, 2009.
[6] L. Valesco, A. P. Vela, F. Morales, and M. Ruiz, "Designing, operating, and reoptimizing elastic optical networks," *J. Lightw. Technol.*, vol. 35, no. 3, pp. 513–526, Feb. 1, 2017.
[7] M. Jinno, B. Kozicki, H. Takara, A. Watanabe, Y. Sone, T. Tanaka, and A. Hirano, "Distance-adaptive spectrum resource allocation in spectrum-slices elastic optical path networks," *IEEE Commun. Mag.*, vol. 48, pp. 138–145 Aug. 2010.
[8] H. Beyranvand and J. A. Salehi, "A quality-of-transmission aware dynamic routing and spectrum assignment scheme for future elastic optical networks," *J. Lightw. Technol.*, vol. 31, no. 18, pp. 3043–3054, Sep. 15, 2013.
[9] M. Moharrami, A. Fallahpour, H. Beyranvand, and J. A. Salehi, "Resource allocation and multicast routing in elastic optical networks," *IEEE Trans. Commun.*, vol. 65, no. 5, pp. 2101–2113, May 2017.
[10] M. Ruiz and L. Velasco, "Serving multicast requests on single-layer and multilayer flexgrid networks," *J. Opt. Commun. Netw.*, vol. 7, no. 3, pp. 146–155, Feb. 2015.
[11] L. Gong, X. Zhou, X. Liu, W. Zhao, W. Lu, and Z. Zhu, "efficient resource allocation for all optical multicasting over spectrum Sliced optical networks," *J. Opt. Commun. Netw.*, vol. 5, no. 8, pp. 836–847, Aug. 2013.
[12] K. Walkowiak, R. Goscien, M. Klinkowski, and M. Wozniak, "Optimization of multicast traffic in elastic optical networks with distance-adaptive transmission," *IEEE Commun. Lett.*, vol. 18, no. 12, pp. 2117–2120, Dec. 2014.
[13] M. Ruiz and L. Velasco, "Performance evaluation of light-tree schemes in flexgrid optical networks," *IEEE Commun. Lett.*, vol. 18, no. 10, pp. 1731–1734, Oct. 2014.
[14] Z. Fan, Y. Li, G. Shen, and C.-K.-C. Chan, "Distance-adaptive spectrum resource allocation using subtree scheme for all-optical multicasting in elastic optical networks," *J. Lightw. Technol.*, vol. 35, no. 9, pp. 1460–1468, May 1, 2017.
[15] X. Li, L. Zhang, Y. Tang, J. Guo, and S. Huang, "Distributed sub-tree-based optical multicasting scheme in elastic optical data center networks," *IEEE Access*, vol. 6, pp. 6464–6477, Jan. 2018.
[16] L. Yang, L. Gong, F. Zhou, B. Cousin, M. Molnar, and Z. Zhu, "Leveraging light forest with rateless network coding to design efficient all-optical multicast schemes for elastic optical networks," *J. Lightw. Technol.*, vol. 33, no. 18, pp. 3945–3955, Sep. 15, 2015.
[17] F. M. Madani, "Scalable framework for translucent elastic optical network planning," *J. Lightw. Technol.*, vol. 34, no. 4, pp. 1086–1097, Feb. 15, 2016.
[18] X. Wang, M. Brandt-Pearce, and S. Subramaniam, "Impact of wavelength and modulation conversion on translucent elastic optical networks using MILP," *IEEE/OSA J. Opt. Commun. Netw.*, vol. 7, no. 7, pp. 644–655, Jul. 2015.
[19] I. Cerutti, F. Martinelli, N. Sambo, F. Cugini, and P. Castoldi, "Trading regeneration and spectrum utilization in code-rate adaptive Flexi-grid networks," *J. Lightw. Technol.*, vol. 32, no. 23, pp. 4496–4503, Dec. 1, 2014.
[20] M. Klinkowski and K. Walkowiak, "On performance gains of flexible regeneration and modulation conversion in translucent elastic optical networks with superchannel transmission," *J. Lightw. Technol.*, vol. 34, no. 23, pp. 5485–5495, Dec. 1, 2016.
[21] H. Ding, M. Zhang, B. Ramamurthy, Z. Liu, S. Huang, and X. Chen, "Routing, modulation level and spectrum allocation with dynamic modulation level conversion in elastic optical networks," *Photon. Netw. Commun.*, vol. 28, no. 3, pp. 295–305, Jun. 2014.
[22] A. Fallahpour, H. Beyranvand, S. A. Nezamalhosseini, and J. A. Salehi, "Energy efficient routing and spectrum assignment with regenerator placement in elastic optical networks," *J. Lightw. Technol.*, vol. 32, no. 10, pp. 2019–2027, May 15, 2014.
[23] A. Bocoi, M. Schuster, F. Rambach, M. Kiese, C.-A. Bunge, and B. Spinnler, "Reach-dependent capacity in optical networks enabled by OFDM," in *Proc. Opt. Fiber Commun. Conf. Nat. Fiber Optic Eng. Conf.*, San Diego, CA, USA, 2009, pp. 1–3.
[24] G. N. Rouskas, "Optical layer multicast: Rationale, building blocks, and challenges," *IEEE Netw.*, vol. 17, no. 1, pp. 60–65, Jan. 2003.
[25] J. Wang, X. Qi, and B. Chen, "Wavelength assignment for multicast in all-optical WDM networks with splitting constraints," *IEEE/ACM Trans. Netw.*, vol. 14, no. 1, pp. 169–182, Feb. 2006.
[26] *Gurobi 8.0.* Accessed: 2020. [Online]. Available: http://www.gurobi.com
[27] Z.-H. Fu, S.-B. Chen, Y.-F. Ming, Y.-Q. Chen, and X.-J. Lai, "Dynamically reconstructing minimum spanning trees after swapping pairwise vertices," *IEEE Access*, vol. 7, pp. 16351–16363, Jan. 2019.
[28] P. Guan and J. Wu, "Effective data communication based on social community in social opportunistic networks," *IEEE Access*, vol. 7, pp. 12405–12414, Jan. 2019.
[29] M. Habibi and H. Beyranvand, "Impairment-aware manycast routing, modulation level, and spectrum assignment in elastic optical networks," *J. Opt. Commun. Netw.*, vol. 11, no. 5, pp. 179–189, Jan. 2019.

MEHDI TARHANI (Member, IEEE) received the M.S. degree in electrical engineering from the Shahid Chamran University of Ahvaz, Ahvaz, Iran, in 2014. He is currently pursuing the Ph.D. degree with the Department of the Electrical and Computer Engineering, The University of Texas at San Antonio. His research interests include optical networks, wireless sensor networks, and (free-space) optical communications.

MORAD KHOSRAVI EGHBAL received the Ph.D. degree in electrical engineering from The University of Texas at San Antonio, in 2018. He is currently a Postdoctoral Fellow with Department of the Electrical and Computer Engineering, The University of Texas at San Antonio. His research interests are millimeter wave RoF networks, free-space optical communications, and WDM optical networks for next-generation mobile communication (5G).

MEHDI SHADARAM received the Ph.D. degree in electrical engineering from The University of Oklahoma, in 1984. He joined UTSA as the Chair of the Department of Electrical and Computer Engineering, in the fall of 2003. Prior to joining UTSA, he was the Schellenger Endowed Professor and the Chairman of the Department of Electrical and Computer Engineering, The University of Texas at El Paso (UTEP). He is currently the Briscoe Distinguished Professor with the Department of Electrical and Computer Engineering, The University of Texas at San Antonio (UTSA). He has extensive experience in obtaining and successfully directing engineering grants. He has been either PI or Co-PI on numerous grants and contracts, totaling more than $10 million in the past 20 years. NASA, the Jet Propulsion Laboratory, the National Science Foundation, the Office of Naval Research, the Department of Defense, the Department of Energy, and the Texas Instruments and Lucent Technologies have funded his research projects. His main area of research activity is in the broadband analog and digital fiber optic communication systems and photonic devices. He has published more than 100 and 40 articles in refereed journals and conference proceedings. Under his supervision, 14 Ph.D. candidates and 38 master's students have finished their degree programs in the past 20 years. Dr. Shadaram was a recipient of numerous awards, including Robert and Maude Gledden Visiting Senior Fellowship Award from the University of Western Australia, the UTSA's President's Distinguished Achievement Award for Excellence in Community Engagement, the UTSA's College of Engineering Excellence in Engineering Research Award, the Best Teacher Award in the College of Engineering, UTEP, and NASA Monterey Award for contribution to the space exploration. He has been the General Chair, the TPC Chair/Member, the Session Chair, and the Panelist in several IEEE conferences. He is also the wireless communications Area Editor of the *Journal of Computers and Electrical Engineering*. He has served on several review boards, including the National Research Council Ford Foundation, the National Science Foundation, the Department of Defense SMART Scholarship Evaluation Panel, the U.S. Civilian Research and Development Foundation, and the Natural Sciences and Engineering Research Council of Canada. He has collaborated with numerous researchers from Japan, France, Canada, and USA, on projects dealing with fiber optic links and devices. He is also a Registered Professional Engineer in the State of Texas.